Supplement of Atmos. Meas. Tech., 11, 6389–6407, 2018
https://doi.org/10.5194/amt-11-6389-2018-supplement

Atmospheric Measurement Techniques
Open Access
EGU

Supplement of

Instrument artifacts lead to uncertainties in parameterizations of cloud condensation nucleation

Jessica A. Mirrielees and Sarah D. Brooks

Correspondence to: Jessica A. Mirrielees (jmirrielees@tamu.edu)

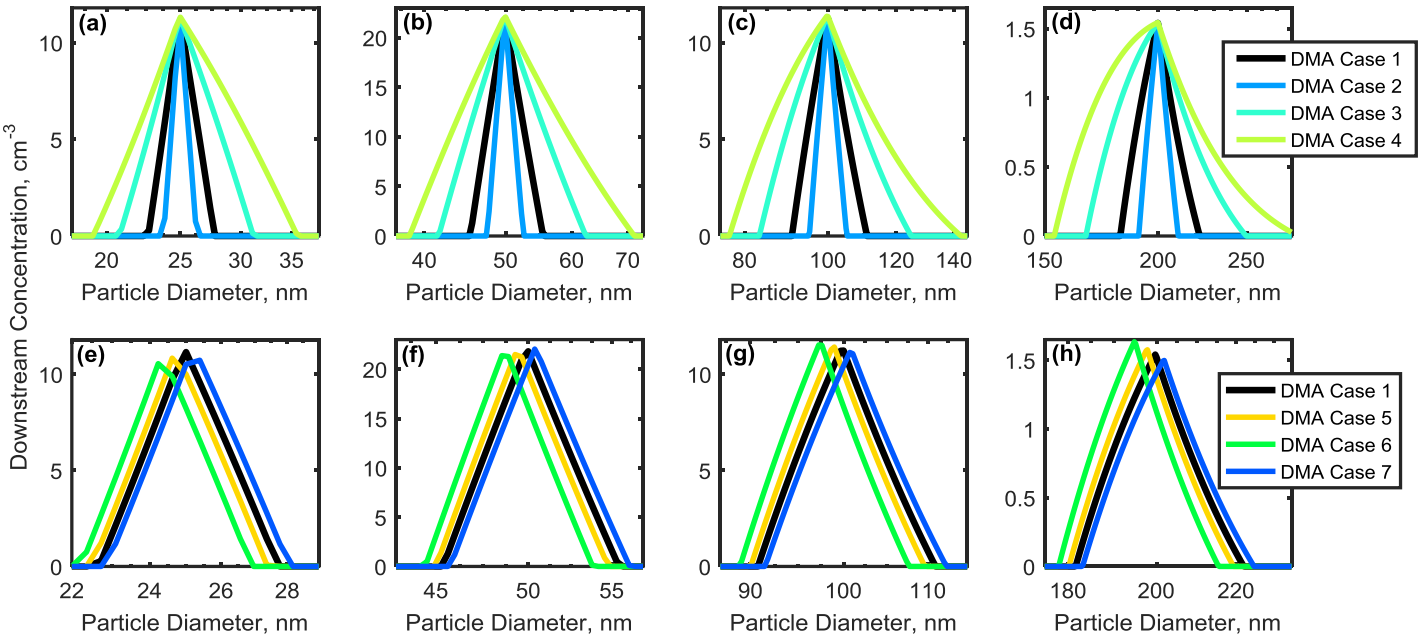

Figure S1 (a-d) Downstream aerosols concentrations, cm^{-3}, for DMA Cases 1-4, with sheath and excess air flow 3 L min^{-1}, and aerosol and sample flow of 0.06-0.90 L min^{-1}. (e-h) Downstream concentrations for DMA Cases 1 and 5-7, with sheath air flow 3.0 L min^{-1}, sample flow 0.30 L min^{-1}, and excess air flow 2.94-3.06 L/min.

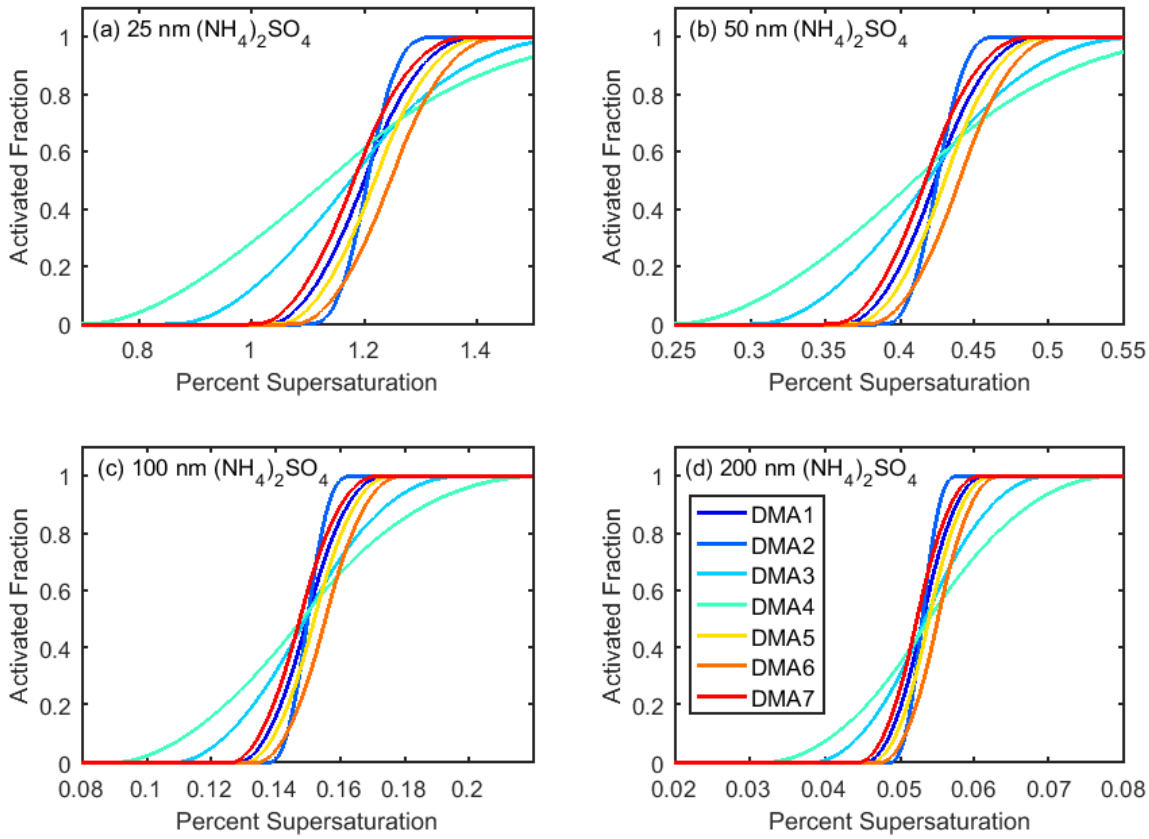

Figure S2 Exemplary $(NH_4)_2SO_4$ CCN activation curves for DMA Cases 1-7.

CCN instrument calibration with ammonium sulfate and sodium chloride

We have now assessed the effects of calibration with a standard compound on subsequent CCN measurements, given that the DMA flow settings used in the calibration are the same as those used for subsequent measurements. Calibration with a standard will yield new parameters, A and B, for a linear equation that relates percent supersaturation, $\%SS$, to the change in temperature set by the instrument, ΔT_{set}:

$$\Delta T_{set} = (A \times \%SS) + B$$

If the slope A and/or y-intercept B are inaccurate, the instrument will choose ΔT_{set} incorrectly for input percent supersaturation values. In order to model this error, the κ-Köhler theory $\%SS_{crit}$ for 25, 50, 100, and 200 nm ammonium sulfate and sodium chloride was used to determine the "correct" ΔT_{set} for the CCNC, using parameters A and B from a previous CCNC calibration in our lab. These ΔT_{set} were then paired with the $\%SS_{crit}$ for DMA Cases 1-7 determined in Section 3.1.2 κ_{app} artifacts arising from DMA flow ratios, as shown in Figure S3. A linear regression was run for each composition and DMA Case to find new parameters A and B. For clarity, the original ΔT_{set} equation with the original parameters A_0 and B_0 will hereon be referred to as Eq. S1, and the new ΔT_{set} equations for each DMA Case C with new parameters A_C and B_C will be referred to as Eq. S2.

$$\Delta T_{set} = (A_0 \times \%SS) + B_0 \quad (S1)$$

$$\Delta T_{set} = (A_C \times \%SS) + B_C \quad (S2)$$

For each composition (sodium chloride or ammonium sulfate) and DMA Case, Eq. S2 was used to determine the ΔT_{set} that the CCNC would set to achieve a series of percent supersaturations (0.01-1.5%). Then, Eq. S1 was used to determine the actual percent supersaturation that would result from each ΔT_{set}. A few assumptions have been made so far: first, that the DMA aerosol/sheath ratio that was used during the calibration is also used in order to collect CCN activation data later, using the same compound; and second, that the original A_0 and B_0 used Eq. S1 were correct.

Two activated fraction curves were then plotted for each DMA Case (an example with DMA Cases 1-4 is shown in Figure S4). The activated fraction values for both curves were taken from the results in Section 3.1.2 κ_{app} artifacts arising from DMA flow ratios. The accurate percent supersaturation values (dashed lines) were obtained from the original equation, and the observed percent supersaturation values (solid lines) are the values that would be reported by the CCNC according to the new equations.

Then, $\%SS_{crit}$ was determined for each observed activated fraction curve, as shown in Fig. S5a. The apparent hygroscopicity κ_{app} was calculated for each DMA Case using Eq. 4, as shown in Fig. S5b. Apparent hygroscopicity artifacts are shown in Fig. S5c-d.

Therefore, errors encountered while calibrating the CCN instrument presents another source of instrument-derived artifacts that may occur when making CCN activation measurements. Errors introduced through calibration with non-ideal DMA flow ratios have been assessed in the Supplement to this study.

The results of this analysis are shown in Fig. S3, S4, and S5. In short, the consequences of calibration with the aerosol and sheath flows in DMA Cases 1-7 on subsequent CCN measurements was assessed, assuming that the same aerosol and sheath flows would be used in these subsequent measurements.

For DMA Cases 1 and 2, κ_{app} artifacts showed negligible change from the previous results (<1% of $\kappa_{app}^{(NH_4)_2SO_4}$ and κ_{app}^{NaCl}). For DMA Cases 3 and 4, κ_{app} artifacts decreased for 25, 50, and 100 nm particles, but increased for 200 nm particles (from -0.9% to 5% of $\kappa_{app}^{(NH_4)_2SO_4}$ and κ_{app}^{NaCl}, and -2% to 13% of $\kappa_{app}^{(NH_4)_2SO_4}$ and κ_{app}^{NaCl}, respectively).

For DMA Cases 5 and 6, κ_{app} artifacts decreased slightly in magnitude, and became positive, whereas κ_{app} artifacts increased in DMA Case 7 and became negative. These results indicate that calibration and data collection will be the most effective when operating the DMA with a low aerosol/sheath ratio, and equal sheath and excess air flows (as in DMA Cases 1 and 2).

The actual effect of CCN instrument calibration with a standard will vary depending on DMA flows, and may also vary with aerosol samples. These results are not meant to take every possible measurement scenario into account. Rather, this analysis illustrates that instrument settings impact CCN measurement certainty in a complex manner.

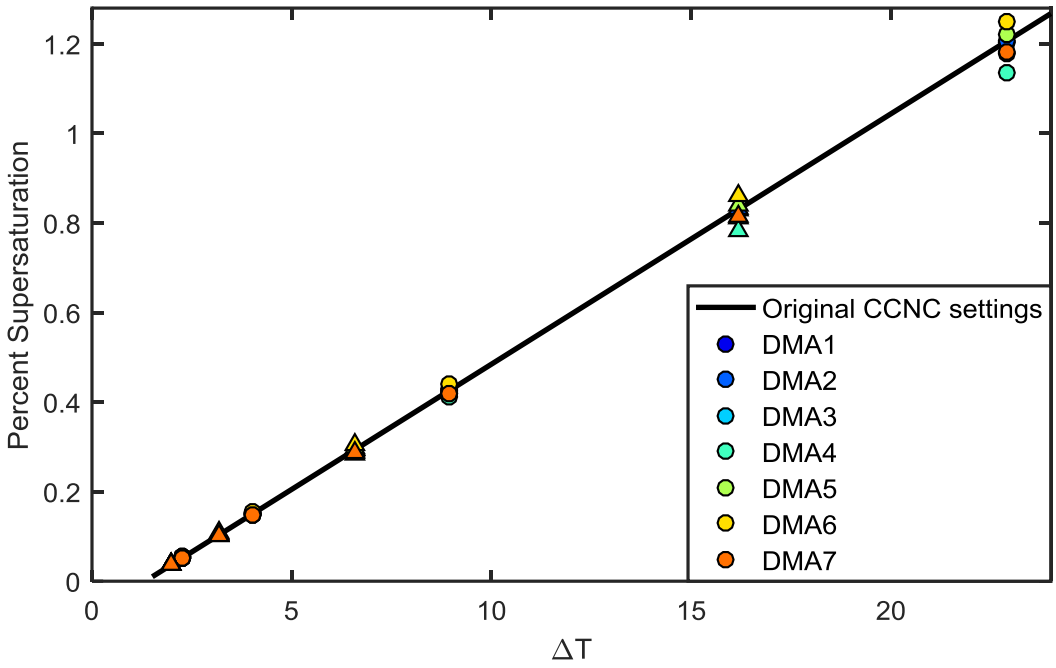

Figure S3 CCN data used to determine new parameters during calibration with $(NH_4)_2SO_4$ (circles) and NaCl (triangles) as standard compounds.

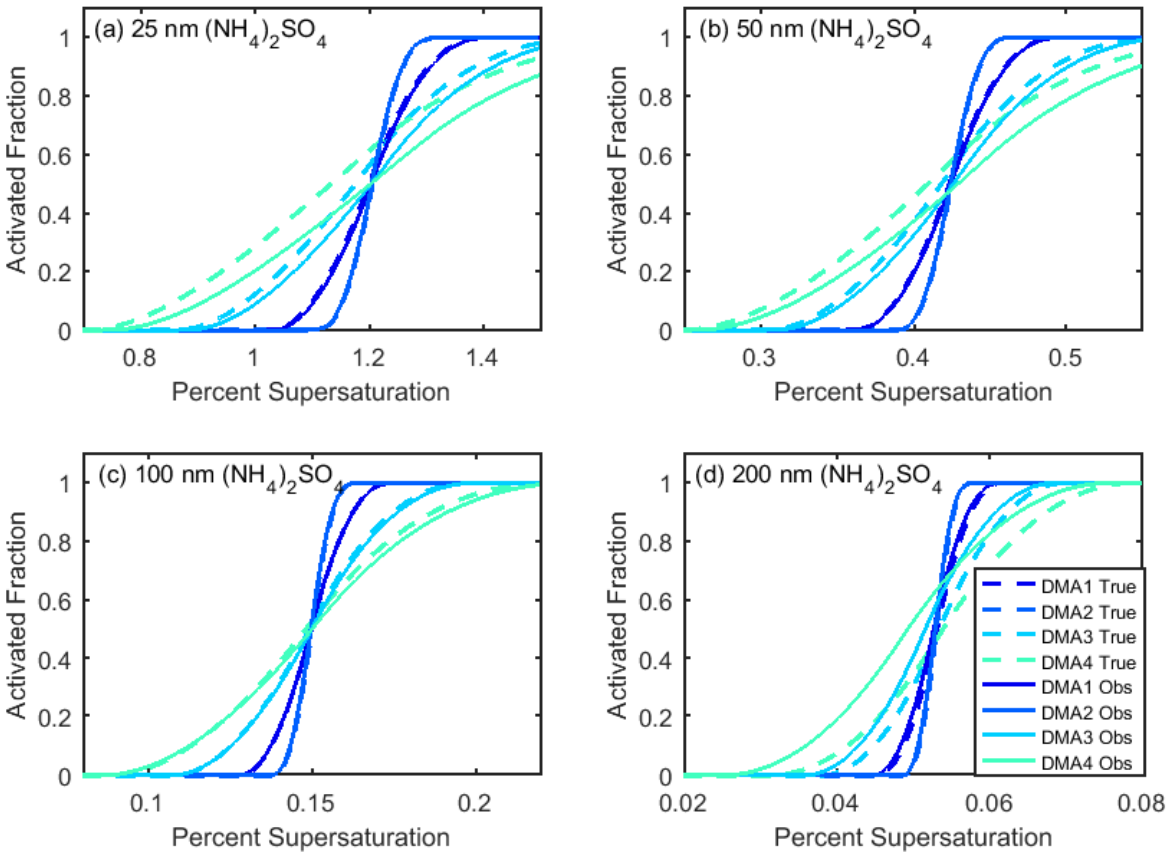

Figure S4 Exemplary $(NH_4)_2SO_4$ CCN activation curves for DMA Cases 1-7, resulting from inaccurate CCN instrument calibration. The true activation curve is shown with dashed lines, and the observed activation (inaccurate supersaturation reported by the instrument) is shown with solid lines.

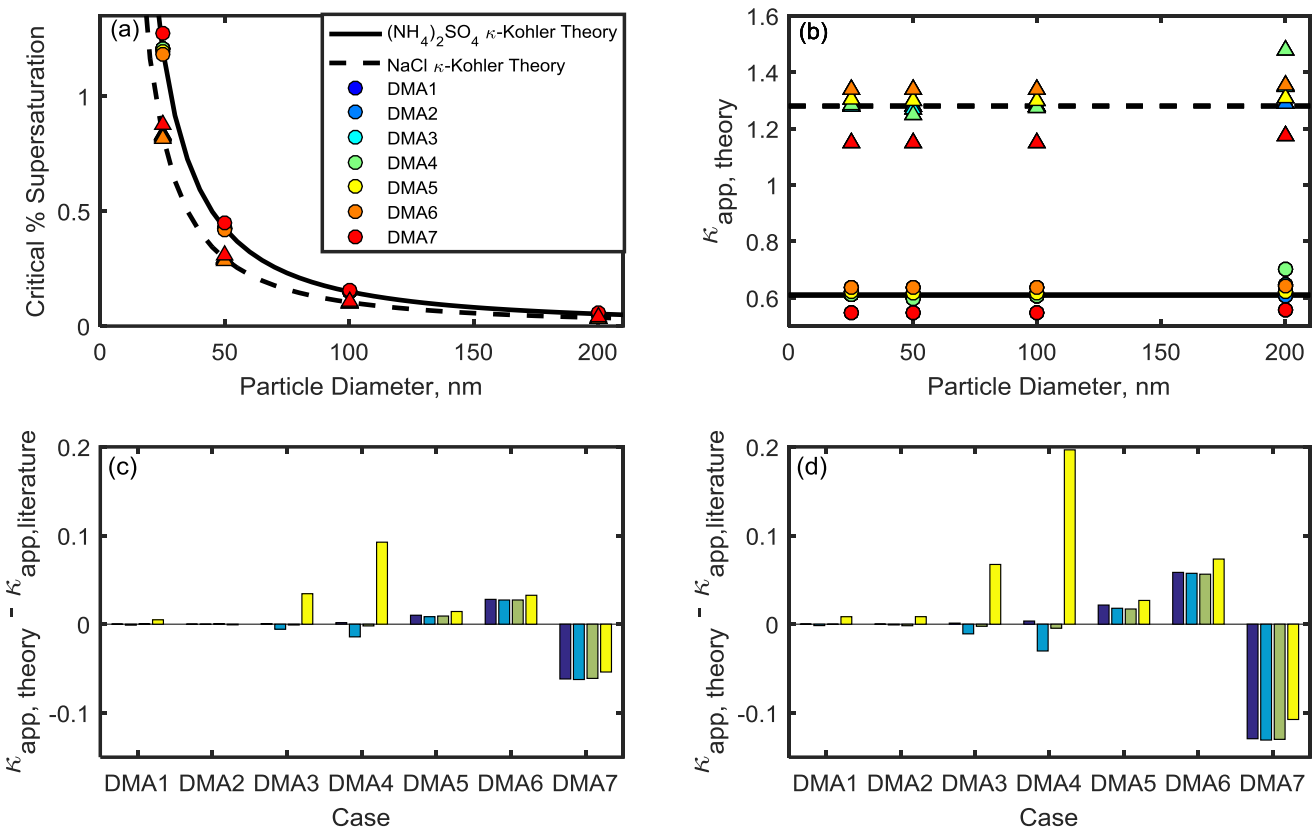

Figure S5 (a) Critical supersaturation of ammonium sulfate and sodium chloride particles calculated for DMA Cases 1-7 for sodium chloride (triangles) and ammonium sulfate (circles), following calibration with the same DMA settings. Ammonium sulfate and sodium chloride curves from κ-Köhler theory are shown for comparison. (b) Apparent hygroscopicity κ_{app} for DMA cases 1-7. (c) DMA-flow-derived artifacts in ammonium sulfate κ_{app} are shown for each DMA case. (d) DMA-flow-derived artifacts in sodium chloride κ_{app} are shown for each DMA case.

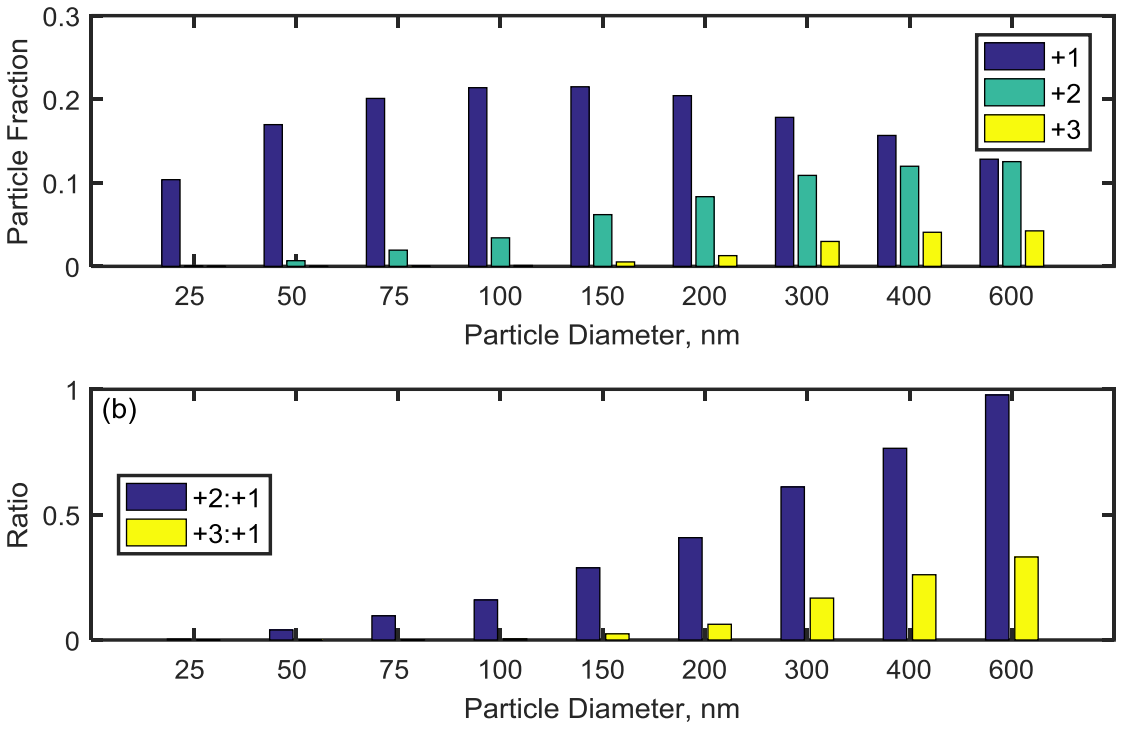

Figure S6 (a) Stationary charge distribution on particles shown in Fig. 3a. The particle diameters were chosen to represent particles that would be present due to single, double, and triple charging for the DMA selected diameters 25, 50, 100, and 200 nm. (b) Ratio of multiple charged particles to single charged particles.